Published by :
http://www.ijert.org

International Journal of Engineering Research & Technology (IJERT)
ISSN: 2278-0181
Vol. 6 Issue 01, January-2017

Parametric Study on CFST Column – Steel Beam Connection Under Cyclic Loading

Akhila Unnikrishnan
M tech scholar: Department of Civil Engineering
N S S College of Engineering,
Palakkad, India

P Asha Varma
Professor: Department of Civil engineering
N S S College of Engineering
Palakkad, India

***Abstract*— This paper deals with the finite element modelling of a CFST column- steel I beam connection with external diaphragm (external stiffener) in ANSYS. Five finite element models of CFST column – steel beam connection with different tube thickness are modeled and named as J1, J2, J3, J4 and J5. The models are analysed under a constant axial load on the CFST column and a cyclic load at the steel beam. The stress distribution in the diaphragm, column, and in the steel beam is studied in different cycles. As the steel tube thickness of CFST column increased there is a considerable reduction in the area under different stress range in steel tube. The maximum compressive principal stress in concrete is reduced due to the increased confinement provided by the steel tube. In the entire five models the failure was reported in the beam indicating a weak beam strong column connection**

Keywords*— Concrete filled steel tubular column, Finite element, ANSYS

I. INTRODUCTION

Concrete Filled Steel Tubular Columns have been used in buildings and bridges. Research had been reported on CFST in countries like China, USA, and Australia since 1970. It consists of an inner concrete core and outer steel tube. They are widely used as compression members in high rise buildings, bridge and underground structures because of their better fire resistance, good performance and lower cost of construction. With the application of CFST column into engineering practices different types of connection have been developed. Rigid connection with transverse stiffeners are commonly used and include external diaphragm connection, internal diaphragm connection and through plate connection.
In this paper CFST column – steel beam connection with external diaphragm connection are modelled and analysed using finite element software. A typical external diaphragm connection used for CFST column is shown in Figure 1.
Studies are reported on CFST column steel beam connection by various researchers since 1980 [1.2.3.4.5.6 etc]. Cyclic load tests are adopted by many researchers to determine the efficiency of the connection. In 2005 Park J W et.al [8] conducted an experimental study on the cyclic performance of wide flange beam square concrete filled tube columns joint with stiffening plates around the column and also described the force transfer mechanism of the connection. Jianguo et.al [5] conducted a finite element modelling and analysis of concrete filled square tubular columns and steel –concrete composite beam in ANSYS. Behaviour of steel beam to concrete filled square and circular column in frames under cyclic loading in beam are reported by Lin Hai Hana et.al [4,6] using a finite element model. Parametric studies to determine the effect of axial load ratio and beam to column linear stiffness ratio are also presented in the paper. In 2012 Daxu zhang et.al [2] conducted an experimental study on the behaviour of column with external stiffener under constant axial load on the column and with cyclic loading at the beam end. Two representative assembly of exterior and interior joint are analysed to determine its seismic characteristics as well as the failure pattern.

This paper presents a finite element models for exterior joint of a CFST column and steel beam with external diaphragms. The models are used to investigate the effect of thickness of steel tube on the stress distribution of the connection under applied cyclic displacement at beam end. The modelling was done in ANSYS 16.2.

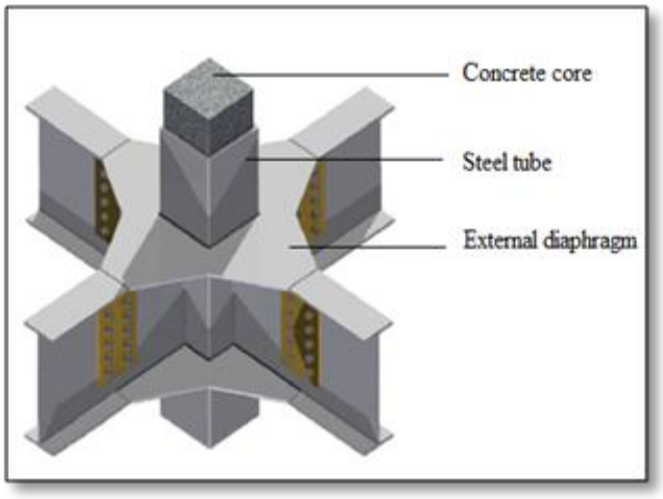

Fig. 1. External diaphragm connection

International Journal of Engineering Research & Technology (IJERT)
ISSN: 2278-0181
Vol. 6 Issue 01, January-2017

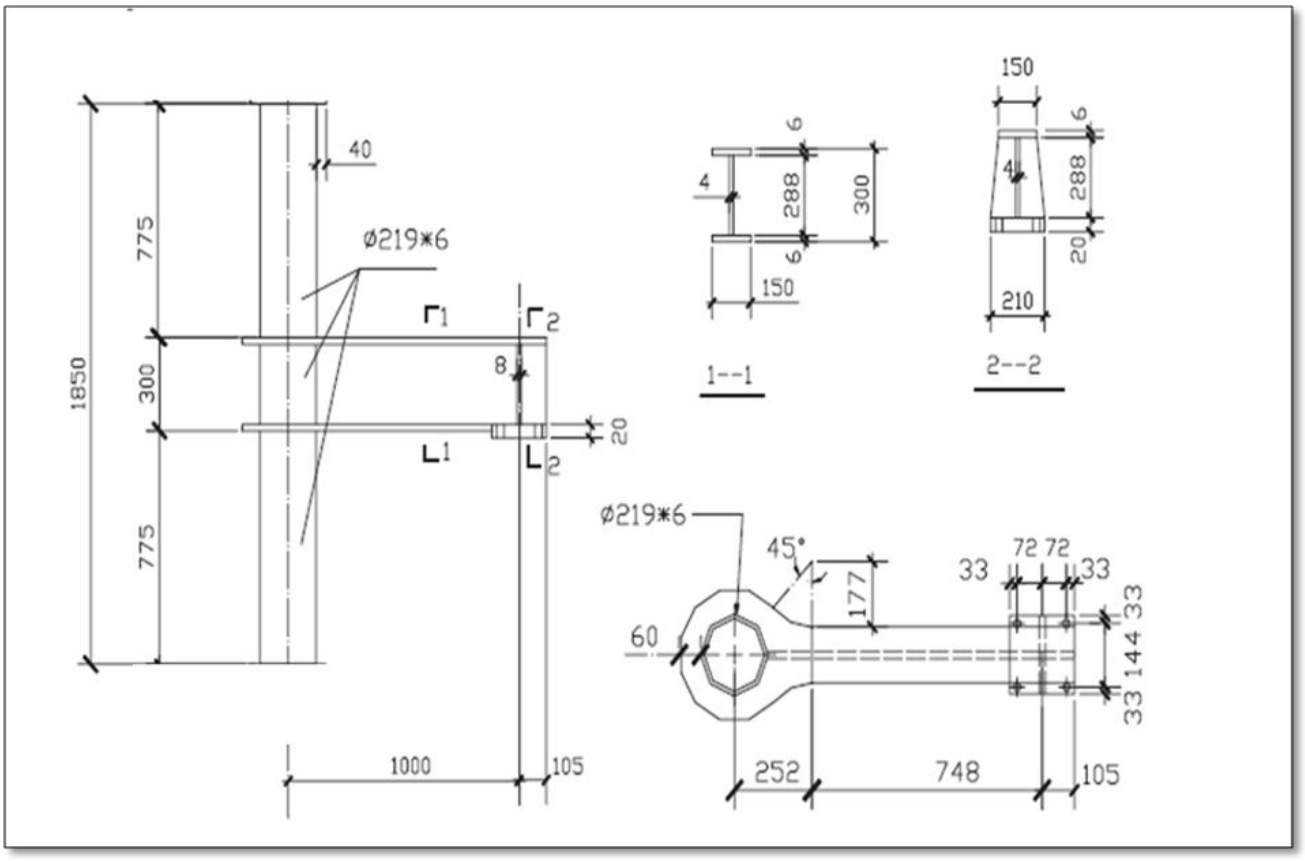

Fig. 2. Geometry of the connection

II. FINITE ELEMENT MODEL

A. *Geometry of the connection*

The exterior CFST column to steel beam connection consist of a circular Concrete filled steel column of diameter 219 mm with a tube thickness of 6mm. A 60 mm wide circular diaphragm of thickness 6mm is used to connect the steel beam. At the point where cyclic displacements are applied stiffeners are provided. The detailed geometry of every part in the connection is given in the figure 2. The geometry is adopted from the experimental study conducted by Daxu et.al [2].

B. *Material Model*

The isotropic hardening model is selected for concrete. SOLID65 element with multi-linear stress-strain curve is employed for modelling concrete in the FEA. The confined uniaxial stress-strain curve is applied to define the concrete material property. Tests have been shown that the stress strain relationship for concrete confined by suitable arrangement is different from that of unconfined concrete. For the CFST column a general stress strain curve for confined concrete is suggested by Liang and Fargomeni [8] is used and is shown in figure 3.

In this curve the stress in the initial region OA is calculated based on the equation given by Mander as

$$\sigma_c = \frac{f'_{cc}\lambda(\varepsilon_c/\varepsilon'_{cc})}{\lambda - 1 + (\varepsilon_c/\varepsilon'_{cc})} \quad (1)$$

$$\lambda = \frac{E_c}{E_c - 1 + (f'_{cc}/\varepsilon'_{cc})} \quad (2)$$

in which,

E_c: Youngs modulus of concrete

σ_c: Compressive concrete stress

f'_c : Cylinder compressive strength of concrete

f'_{cc}: Effective compressive strength of confined concrete

γ_c: Strength reduction factor

ε_c: Compressive concrete strain corresponding to f'_c

ε'_{cc} :Concrete strain corresponding to f'_{cc}

The young's modulus of concrete is given by,

$$E_c = 3320\sqrt{\gamma_c f'_c} + 6900 \text{ (MPa)} \quad (3)$$

International Journal of Engineering Research & Technology (IJERT)
ISSN: 2278-0181
Vol. 6 Issue 01, January-2017

The confined concrete strength is given by,

$$f'_{cc}=\gamma_c f'_c+k_1 f_{rp} \quad (4)$$

The concrete strain corresponding to f'_{cc} is given by,

$$\varepsilon'_{cc}=\varepsilon'_c\left(1+k_2\frac{f_{rp}}{\gamma_c f'_c}\right) \quad (5)$$

Where f_{rp} is the lateral confining pressure on the concrete by the steel tube and k_1 and k_2 are taken as 4.1 and 20.5 respectively.

The parts AB and BC of the stress–strain curve shown in Figure 3 can be described by the following equations

$$\sigma_c=\begin{cases}\beta_c f'_{cc}+\left(\frac{\varepsilon_{cu}-\varepsilon_c}{\varepsilon_{cu}-\varepsilon'_{cc}}\right)\left(f'_{cc}-\beta_c f'_{cc}\right) & \text{for } \varepsilon'_{cc}<\varepsilon_c\le\varepsilon_{cu}\\ \beta_c f'_{cc} & \text{for } \varepsilon_c>\varepsilon_{cu}\end{cases} \quad (6)$$

where ε_{cu} is taken as 0.02 as suggested by Liang and Fragomeni [8] based on the experimental results, and βc is a factor accounting for the confinement effect by the steel tube on the post-peak strength and ductility of the confined concrete, which is given by Hu et al. as

$$\beta_c=\begin{cases}1.0 \text{ for } \frac{D}{t}\le 40\\ 0.0000339\left(\frac{D}{t}\right)^2-0.010085\left(\frac{D}{t}\right)+\\ 1.3491 \text{ for } 40<\frac{D}{t}\le 150\end{cases} \quad (7)$$

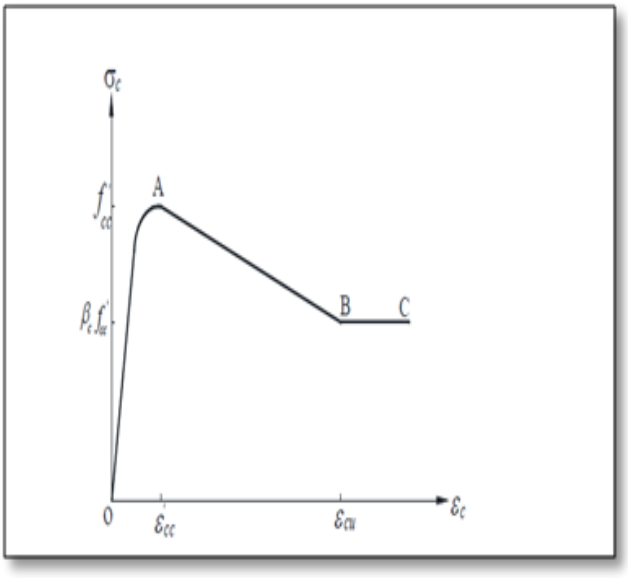

Fig. 3. Stress-strain curve for confined concrete

The above equations are used to develop the multi-linear stress strain curve in the finite element modelling of the concrete with an unconfined cube compressive strength of 27.5 MPa. The Poisson's ratio of concrete is taken as 0.2.

$$E'=E_{st}\exp\left(-\xi\frac{\varepsilon-\varepsilon_{st}}{\varepsilon_y}\right)$$

$$\frac{\sigma}{\sigma_y}=\frac{1}{\xi}\frac{E_{st}}{E}\left[1-e^{-\xi\left(\varepsilon/\varepsilon_y-\varepsilon_{st}/\varepsilon_y\right)}\right]$$

Material	ξ	E/E_{st}	$\varepsilon_{st}/\varepsilon_y$
SS400	0.06	40	10
SM490	0.06	30	7
SM570	0.02	100	3

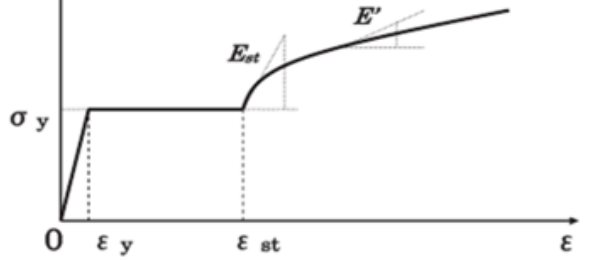

Fig. 4. Stress – strain curve for stee

The behaviour of steel was modelled by a nonlinear kinematic hardening model using SOLID186 element. Uniaxial stress–strain curve adopted is shown in Figure 4. The model considers the strain hardening of the steel. The elastic properties, Young's modulus, E and Poisson's ratio, ν were set to be 206 GPa and 0.3, respectively

The commencement of plastic deformation in steel is predicted by von-Mises yield criterion. The von-Mises yield criterion defines the equivalent von-Mises stress σ_e which is compared with the characteristic yield strength of material to predict yielding.

The material properties of the steel specimens used in the connection is given in Table 1.

TABLE I. GEOMETRICAL AND MATERIAL PROPERTIES OF SPECIMEN

Specimen		Yield strength (MPa)	Geometry (mm)
I beam	Flange	257	**150×6**
	Web	285	**288×4**
Steel tube		368	**Φ219×6**
Diaphragm		332	**60×6**

C. Concrete to Steel Interface Modelling

The interaction between concrete and steel tube at the interface was modeled using contact elements. The outer surface of concrete and inner surface of the steel tube was

International Journal of Engineering Research & Technology (IJERT)
ISSN: 2278-0181
Vol. 6 Issue 01, January-2017

specified to give a frictional contact. The classical isotropic Coulomb friction model was used to model the interaction assuming the coefficient of friction as 0.6. CONTACT174 and TARGE170 elements are used for modelling this contact.

D. Applied Displacements and Loading

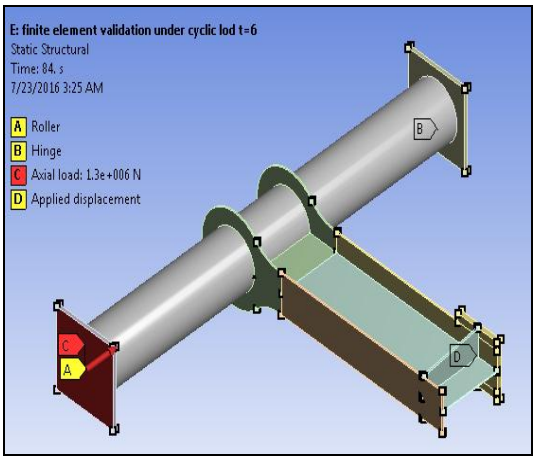

Fig. 5. Applied boundary condition, load and displacement

In this model boundary conditions are applied to the top and bottom of the CFST column. At the top surface the displacement in X and Y direction are constrained and at the bottom surface the displacement in X, Y and Z direction are constrained.

An axial compressive load is applied in the column and cyclic displacements are applied at the beam end. The axial compressive load applied to the column was 1300 kN and was kept constant for the whole loading process. Then a cyclic displacement is applied in the beam end the loading pattern is adopted from the experimental study conducted by Daxu et.al in 2012 [2]. The applied displacement and load are given in Figure 5

E. Specification of Model

A total 5 models are developed varying the thickness of the steel tube in the connection. The material properties for steel tube, diaphragm and beam are kept constant. In the concrete core the confined compressive strength will depend on the D/t ratio of the CFST column and is calculated using equations given in section 2.2.

TABLE II. GEOMETRIC SPECIFICATIONS OF MODEL J1 TO J5

Model	Diameter of core concrete (mm)	Thickness of steel tube (t) (mm)	Diameter of diaphragm (mm)	Width of diaphragm (mm)
J 1	207	6	219	60
J 2	207	8	223	60
J 3	207	10	227	60
J 4	207	12	231	60
J 5	207	14	235	60

The finite element model developed was employed to investigate the effects of the thickness of stainless steel tube on the stress distribution in the connection. The five models are named as J1, J2, J3, J4 and J5. And their geometric specifications are given in Table 2.

III. RESULTS AND DISCUSSIONS

A. Stress Distribution in Steel Specimens

For steel the failure criterion adopted is the equivalent von-Mises yield criterion. For concrete the principal stress is compared with the compressive strength of concrete since it is a brittle material.

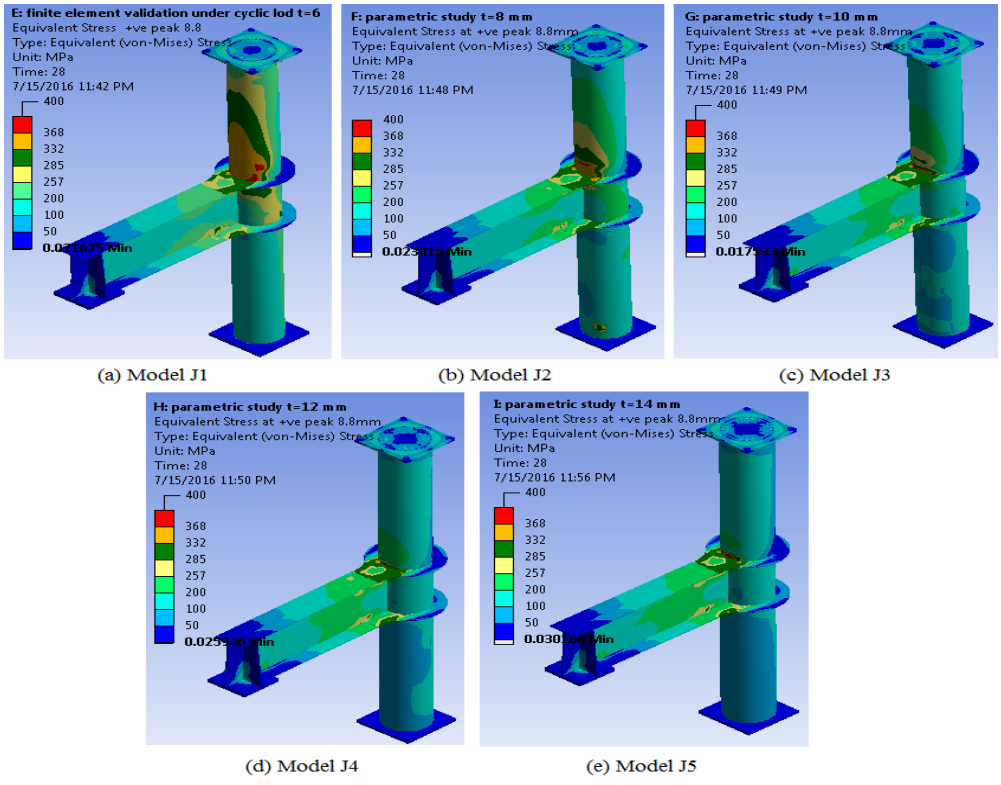

(a) Model J1 (b) Model J2 (c) Model J3

(d) Model J4 (e) Model J5

Fig. 6. Equivalent stress distribution in models J1 –J5 at positive peak of Δy cycle

International Journal of Engineering Research & Technology (IJERT)
ISSN: 2278-0181
Vol. 6 Issue 01, January-2017

In the first displacement control cycle (i.e. Δy cycle), the distribution of equivalent stress at maximum positive displacement in all the five models J1,J2,J3,J4 and J5 is given in figure 6(a) – (e). As the thickness increases the area under each stress range decreases. No yielding of flange, web or stiffener is seen in Models J1- J5. In model J1 the tube was yielded in a small area but it is not penetrated through the entire thickness.

In the next cycle (2Δy) at the positive peak the tube in models J1 the area of under stress range 332 – 368 MPa increased reducing the area under the range 285 -332 MPa. In this cycle the flange region nearer to the diaphragm is yielded. In the web dominant maximum stress range is increased from 200 – 257 MPa to 257 -285 MPa. In addition to this a small region in the web near to the yielded flange has observed with an equivalent stress range greater than yield stress of web. Models J3, J4 and J5 are not yielded except in the flange of the beam. In model J2 and J3 there is an increase in area under all the stress range comparing with that in the Δy cycle but is less than that of Model J1. The interesting fact is that in Model J4 and J5 the increased deflection in the 2Δy cycle couldn't make significant increase in the stress in the steel tube. When comparing the models in Δy and 2Δy cycle, the flange in the steel beam is yielded in 2Δy cycle and it was not yielded in the Δy cycle. Another difference is the increase in area under various stress range, however this increase in stress is negligible in model J4 and J5. The description given above about the equivalent stress distribution can be easily understood with the help of figure 7(a) – (e)

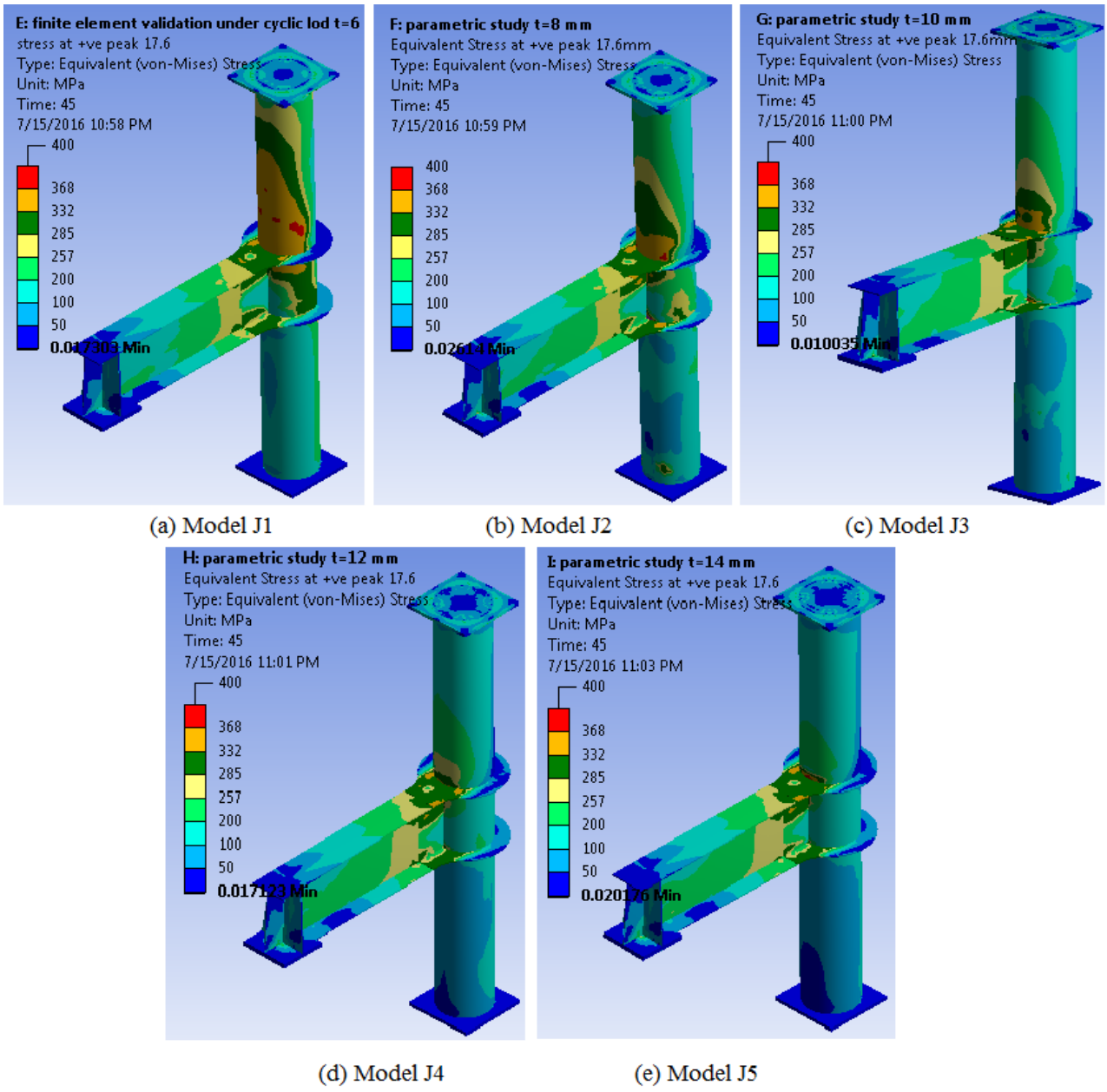

(a) Model J1 (b) Model J2 (c) Model J3

(d) Model J4 (e) Model J5

Fig. 7. Equivalent stress distribution in models J1-J5 at positive peak of 2Δy cycle

International Journal of Engineering Research & Technology (IJERT)
ISSN: 2278-0181
Vol. 6 Issue 01, January-2017

In the last cycle the yielding is extended to the whole depth of steel beam in all the five models..This significant yielding indicates a plastic hinge formation near to the beam diaphragm joint. In the top and bottom flange of Diaphragm equivalent stress exceeded the yield stress near to the beam stiffener joint in all the five models. Only in model J1equivalent stress exceeded the yield strength of steel tube. In model J4 and J5 the stress induced in tube is very much less than its yield strength and largest part of tubes are under the stress range of 100 -200 MPa. So as the thickness of steel tube increases the failure of beam will occur first avoiding the possibility of column failure.

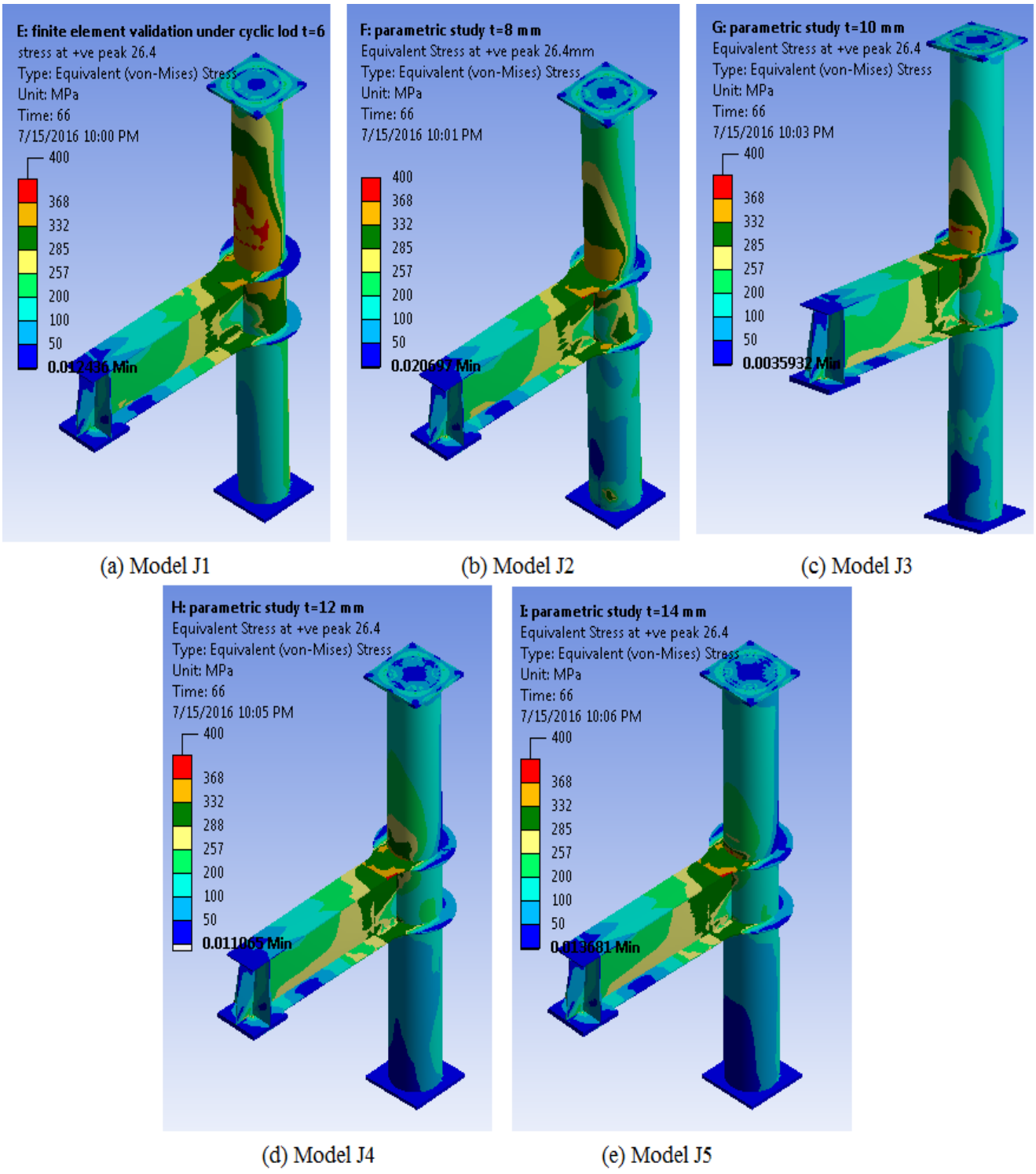

(a) Model J1 (b) Model J2 (c) Model J3

(d) Model J4 (e) Model J5

Fig. 8. Equivalent stress distribution in models J1-J5 at positive peak of 3Δy cycle

International Journal of Engineering Research & Technology (IJERT)
ISSN: 2278-0181
Vol. 6 Issue 01, January-2017

B. Stress Distribution in Concrete

In concrete also as the steel tube increase there is a considerable reduction in the maximum compressive principal stress obtained. As the thickness of tube increases, the confinement effect given by the steel tube to the concrete increases.

The maximum value of maximum compressive principal stress obtained in all the three cycle at the maximum positive displacement is given Table 3. The principal stress distribution in the Δy, 2Δy and 3Δy cycle at maximum positive displacement is given in figures 9-11.

From figure 9, it is clear that the maximum stress in concrete core is distributed near to the top flange of the stiffener (Diaphragm). The maximum value of principal stress is -43.681MPa in Model J1 and is greater than the unconfined compressive strength of concrete. In model J2 as the thickness of steel tube increased from 6-8mm the maximum compressive principal stress decreased from -43.681MPa to -34.73MPa. In model J2 (Figure 9 (c)) principal stress again decreased to 29.97MPa. When the thickness of tube is 12mm a stress of -26.615MPa is obtained and a further increase in thickness produced a maximum stress of -25.886 MPa in Model J5. The decrease in principal stress is comparatively less from Model J4 to Model J5.

In the next cycle in which the peak displacement is 2 Δy the principal stress is increased in all the five models comparing to the Δy cycle. There is no considerable increase in the principal stress in Model J5 comparing to the other Models. The stress is increased in J1 from -43.8681 to -57.872, in J2 from -34.73 to -43.362, in J3 from -29.97 to -35.492 and in J4 from -26.615 to -30.803.

TABLE III. COMPARISON OF MAXIMUM COMPRESSIVE PRINCIPAL STRESS IN CONCRETE

Displacement cycle	Model number	Maximum compressive principal stress (MPa)
Δy cycle (Stress at positive peak)	J1	-43.681
	J2	-34.73
	J3	-29.97
	J4	-26.615
	J5	-25.886
2Δy cycle (Stress at positive peak)	J1	-57.87
	J2	-43.62
	J3	-35.492
	J4	-30.803
	J5	-26.943
3Δy cycle (Stress at positive peak)	J1	-67.58
	J2	-50.795
	J3	-39.713
	J4	-33.424
	J5	-27.062

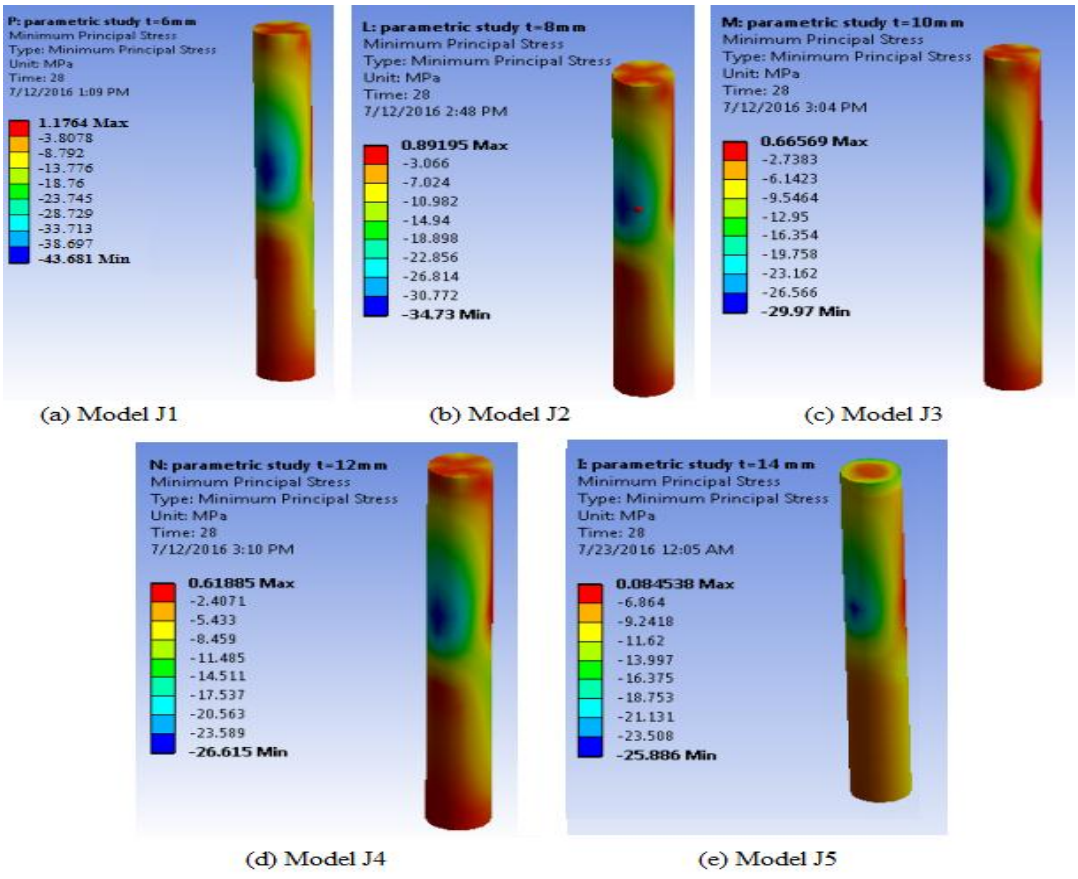

Fig. 9. Maximum compressive principal stress distribution in concrete in the Δy cycle

International Journal of Engineering Research & Technology (IJERT)
ISSN: 2278-0181
Vol. 6 Issue 01, January-2017

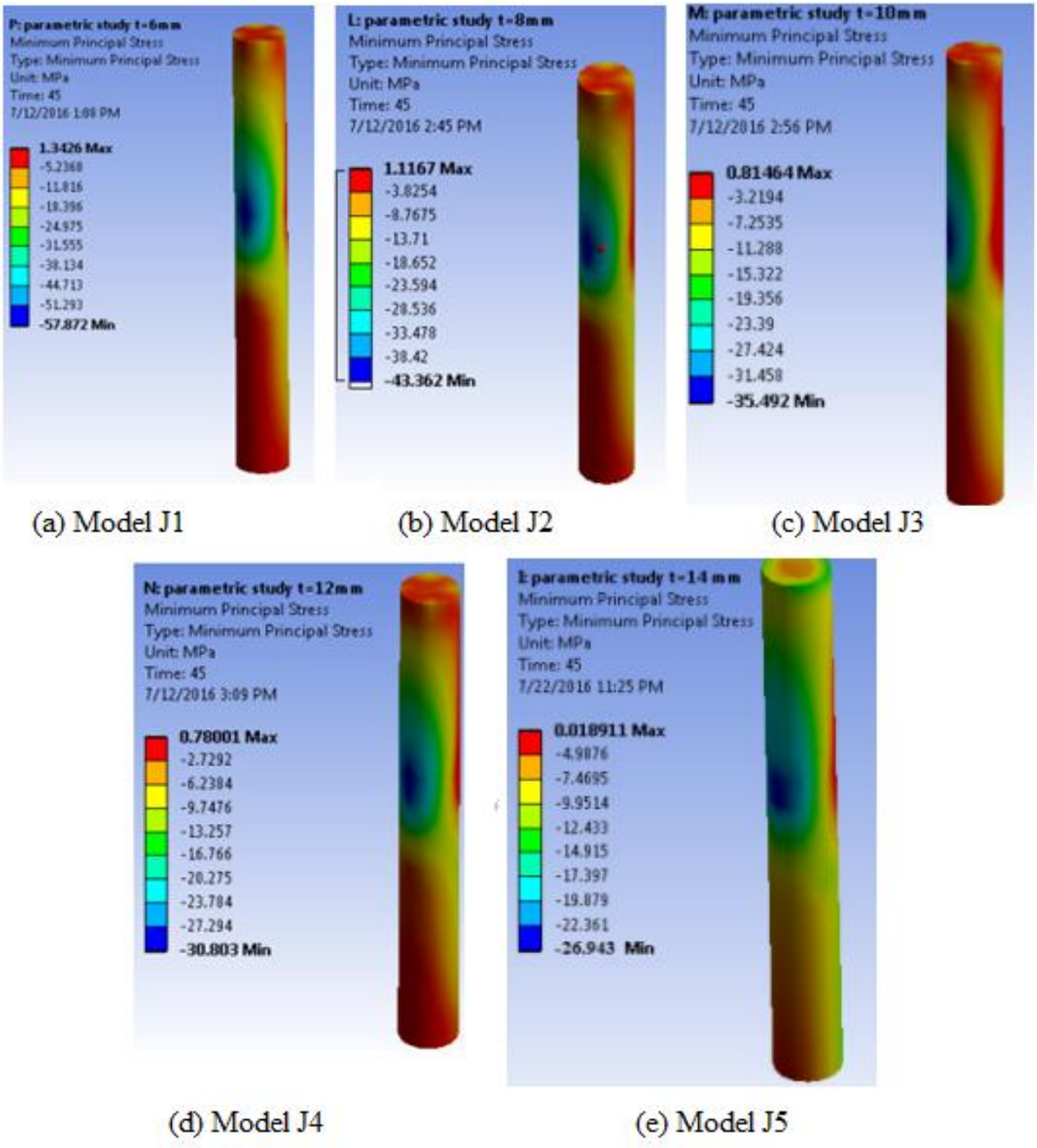

Fig. 10. Maximum compressive principal stress distribution in concrete in the 2Δy cycle

In the last displacement cycle also the principal stress increased from that obtained in the previous cycle. In Model J1, J2, J3 and J4 the increase in stress is significant. But in model J5 the stress is increased but an increase of less than 1 was found.

So it can be concluded that as the tube thickness increases the stress in the tube decreases but it has no significant effect in the stress in diaphragm or beam. The increase in tube thickness is affecting the stress distribution of steel tube and concrete only. The failure is due to the yielding of steel beam.

International Journal of Engineering Research & Technology (IJERT)
ISSN: 2278-0181
Vol. 6 Issue 01, January-2017

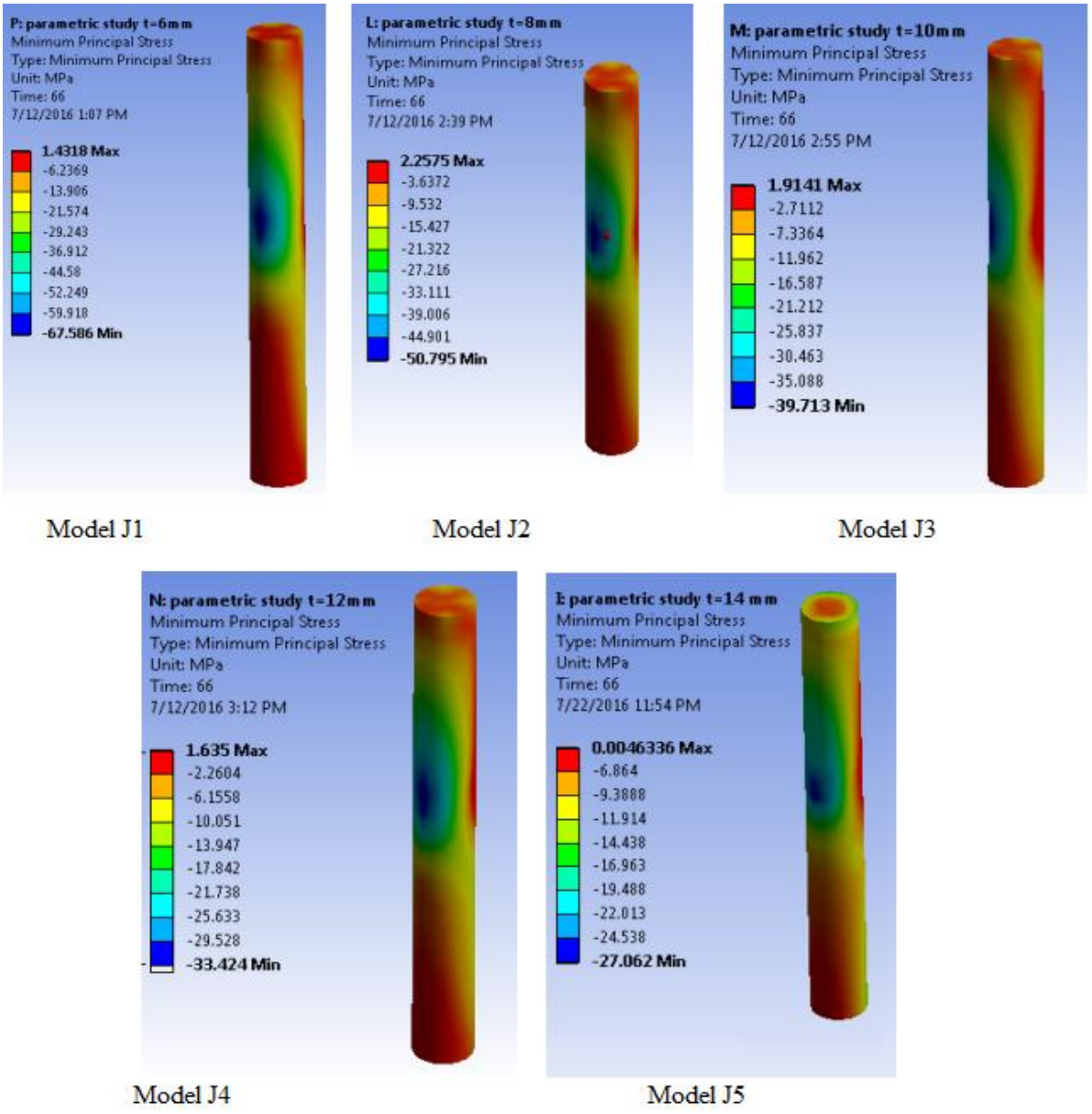

Fig. 11. Maximum compressive principal stress distribution in concrete in the 3Δy cycle

IV. CONCLUSION

- The finite element model in ANSYS developed was able to represent the exterior connection of CFST column and Steel beam with ring stiffener around the column.
- As the thickness of tube increases the area of region yielded in the tube decreases considerably and also the stress induced in concrete decreases. But there is no significant reduction or increase in the stress induced in the diaphragm or beam.
- The beam nearer to the stiffener is yielded first ensuring a strong column weak beam connection
- The thickness of the steel tube in a CFST column – steel beam connection should be selected by reducing the probability of column failure at the same time considering the economy.

The finite element model can be used for parametric studies for determining the effect of axial load ratio, material property, dimension and shape of stiffener etc on the stress distribution as well as on the seismic characteristics.

International Journal of Engineering Research & Technology (IJERT)
ISSN: 2278-0181
Vol. 6 Issue 01, January-2017

REFERENCES

[1] Cui Chunyi, Zhao jinfeng, Zhang Yannian and Zuo Wenxin (2014) " Experimental analysis of mechanical performance of CFST column to assembled steel H- beam connections" The open mechanical Engineering Journal, Vol.8 ,270-278

[2] Daxu Zhang, Shengbin Gao, Jinghai Gon (2012) "Seismic behaviour of steel beam to circular CFST column assemblies with external diaphragms" Journal of Constructional Steel Research

[3] Fei-Yu Liao , Lin-Hai Han,, Zhong Tao (2009). "Seismic behaviour of circular CFST columns and RC shear wall mixed structures: Experiments" Journal of Constructional Steel Research –Vol 67,127-139.

[4] Jianguo Niea, Kai Qinb, C S Caic (2008) "Seismic behavior of connections composed of CFSSTCS and steel–concrete composite beams finite element analysis" Journal of Constructional Steel Research Vol.64 680–688

[5] J W Park, S M Kang and S C Yang (2005) "Experimental studies of wide flange beam to square concrete filled tube column joints with stiffening plates around the column" Journal of Structural Engineering, Vol. 131, No. 12, December 1.

[6] J Y Richard Liew, Mingxiang Xiong (2015) "Design Guide for Concrete Filled Tubular Members with High Strength Materials to Eurocode 4". Research Publishing Singapore.

[7] LH Han, W D Wang, X L Zhao (2008) Behaviour of steel beam to concrete-filled SHS column frames: Finite element model and verifications. Journal of Constructional Steel Research Vol. 30(6):1647_1658

[8] Lin-Hai Han, Wen-Da Wanga, and Xiao-Ling Zhao (2009) "Analytical behavior of frames with steel beams to concrete-filled steel tubular column" Journal of Constructional Steel Research Vol 65 :497_508.

[9] Lin-Hai Han, Wen-Da Wang, Zhong Tao (2011) "Performance of circular CFST column to steel beam frames under lateral cyclic loading" Journal of Constructional Steel Research Vol. 67 876-890.

[10] Vipilkumar Patel, Q. Liang, & M. N. S. Hadi, (2014). "Nonlinear analysis of axially loaded cicular concrete-filled stainless steel tubular short columns". Journal of Constructional Steel Research, 101 (October), 9-18.

[11] Wei Li, Lin-Hai Han (2011) "Seismic performance of CFST column to steel beam joints with RC slab: Analysis" Journal of Constructional Steel Research Vol. 67,127-139.